

Application of Fast Light in Gravitational Wave Detection with Interferometers and Resonators

M.S. Shahriar, M. Salit*

*EECS Department, Northwestern University
Evanston, IL, USA*

In this paper, we study several designs for interferometric gravitational wave detectors, and the potential for enhancing their performance with a fast-light medium. First, we explore the effect of such a medium on designs similar to those already planned for Advanced LIGO. Then we review the zero-area Sagnac interferometer for GW detection, comparing its properties against the more conventional GW detector based on a Michelson interferometer. We next describe a modified version of such a detector where the Sagnac interferometer is replaced by a zero-area Sagnac ring resonator fed by an external laser. We then consider a GW detector based on an active, zero-area Sagnac ring resonator, where a gain medium is present inside the cavity. Finally, we show that if a medium with negative dispersion, which yields the fast-light effect, is also present inside this detector, then its sensitivity to GW strain is enhanced by the inverse of the group index of the dispersive medium. We describe conditions under which this enhancement factor could be as large as 10^5 .

PACS Number(s): 42.50.Ct, 42.50.Gy, 42.60.Da

*Corresponding author. Email: m-salit@northwestern.edu

I. Introduction

It is well accepted that General Relativity predicts the existence of gravitational waves (GWs)¹. The effect of GWs has been observed indirectly, by monitoring the change in the orbital frequency of neutron stars in a binary system (PSR1913+16) as they lose energy via gravitational radiation. However, GWs have not yet been observed directly. The ability to detect GWs routinely will open a new window into the Universe. The attempt to detect GWs using laser interferometry is underway at several observatories. These include the LIGO, the VIRGO, the GEO 600, and the TAMA 300². At the same time, planning is underway for improving the sensitivities of these detectors. For example, the Advanced LIGO system will employ better mirrors, higher laser power, and additional optical components for power and signal recycling^{3,4,5,6,7}. However, even if these detectors are able to see GWs, they will only detect events that produce the strongest signals. There will continue to be a need for detectors that are far more sensitive, in order to detect weaker sources of GW. Furthermore, more sensitive detectors may make the detection of GWs much easier as an engineering project, possibly using configurations that are far more compact than the LIGO type systems.

We have shown⁸ both theoretically and experimentally that incorporating a fast-light medium into an optical cavity can broaden the linewidth of the cavity without correspondingly reducing its finesse. It will, at the same time, cause the resonant frequency of such a cavity to change by a larger amount for a given change in the length of the cavity than the empty cavity case.

To see how the enhanced sensitivity comes about, we recall first how the White Light Cavity (WLC) works in general, configured as a Fabry Perot Cavity (FPC) tuned to resonance, at a frequency f_o , corresponding to a wavelength of λ_o . When the frequency is changed from this value, f_o , the wavelength changes, so that the resonance condition is no longer fulfilled, leading to dephasing and a drop in the intra-cavity intensity and the transmission. Suppose now that a medium with a frequency dependent index, $n(f)$, is placed inside the FPC. The wavelength now is proportional to $1/[fn(f)]$. If $n(f)$ is chosen to depend on f in a manner so that $[fn(f)]$ remains unchanged as a function of f around f_o , then the wavelength remains unchanged at λ_o even when $\Delta f \equiv (f - f_o)$ is non-zero. Under this condition, the cavity will remain resonant over a range of frequencies for which this frequency dependence of $n(f)$ holds. However, the cavity finesse and therefore the build-up factor remain virtually unchanged. The WLC condition requires that $n(f)$ decrease with increasing f , which corresponds to negative dispersion. If the FPC is completely filled with such a dispersive medium, the exact condition for WLC corresponds to a vanishing group index [defined as $\partial(nf)/\partial f$], which is the ratio between free-space speed of light and the group velocity. As such, this leads to an infinite group velocity of light; however, since the condition can remain valid over a finite bandwidth for any real medium, the front edge (corresponding to an infinite bandwidth) can never propagate faster than the free space speed of light⁹, so that there is no violation of special relativity.

The WLC has another important property: it can be used to measure displacement much more sensitively than what can be done with an empty cavity. This enhanced sensitivity of a White Light Cavity (WLC) to mirror displacement or to rotation has been studied experimentally and theoretically by us as well as others^{10,11,12,13,14}.

To see why it works, consider again first an empty FPC, of length L tuned to resonance, at a frequency f_o , corresponding to a wavelength of λ_o , so that $L_o = m\lambda_o/2 = mc/2f_o$, where m is an integer. When the length changes by ΔL , the cavity is no longer resonant. The cavity can be restored to resonance by changing the frequency by $\Delta f = \Delta L / \{(\partial L / \partial f)|_{L_o}\}$. The sensitivity, $S \equiv \Delta f / \Delta L$ is thus given by $1 / \{(\partial L / \partial f)|_{L_o}\}$, which

is easy to calculate from the expression for L given above. Suppose now that a medium with a frequency dependent index, $n(f)$, is placed inside the FPC. The wavelength now is proportional to $1/[fn(f)]$, so that, on resonance, $L_o = m\lambda_o/2 = mc/[2n(f_o)f_o]$. If $[fn(f)]$ remains unchanged as a function of f around f_o , then the wavelength remains unchanged at λ_o . Therefore, within the range over which this condition remains valid, there is no amount of Δf that can restore the cavity to resonance. This implies infinite sensitivity to a mirror displacement. We can also see it formally by noting that $(\partial L/\partial f)|_{L_o}$ vanishes (since the value of L for resonance is unchanged when f changes), which means S becomes infinite. In practice, due to the fact that n is linear in frequency only over a finite range, the value of S remains finite¹⁵. We have shown theoretically¹⁵ and experimentally^{16,17} that the enhancement factor scales as the inverse of the group index. However, for realistic system parameters, the value of S can still be as much as 10^5 times larger than its empty-cavity value.

I. Optical Configurations for Gravitational Wave Detectors

Advanced LIGO is designed to have two modes of operation, a narrowband mode, and a broadband mode. In both modes, the sidebands created on the laser light by gravitational waves undergo multiple reflections within cavities in the arms of the interferometer. In both modes, the arm-end mirror (or end test mass) is one of the mirrors of the cavity, and the other mirror is actually a compound system, comprising one mirror in each arm (the input test mass mirror) and a second mirror in front of the detector (the signal recycling mirror). The compound system is a Fabry-Perot cavity in its own right, known as the signal extraction cavity (SEC). The signal extraction cavity, then, acts as the output coupler for the sidebands leaving the arm cavity, and it has a reflectivity which can be controlled by tuning the relative positions of the input test mass and the signal recycling mirror. The reflectivity of the SEC is frequency dependent, but assuming the resonance bandwidth of the SEC is much larger than the range of relevant gravitational wave frequencies (up to tens of kilohertz), the reflectivity can be approximately the same for the laser frequency and the whole spectrum of potential GW sidebands. If the SEC is tuned to resonate near the laser frequency, its reflectivity is low, whereas if it is detuned away from the laser frequency, it can be highly reflective. The reflectivity of the SEC determines the finesse of the arm cavities, and thus their bandwidth. The detector operates in narrowband mode when the SEC is highly reflective and broadband mode when its reflectivity is low. The sensitivity of the detector is greater in the narrowband mode, but the loss of bandwidth makes it ill suited to detecting some potential gravitational wave sources. The WLC concept eliminates this tradeoff.

B.J. Meers derived the frequency response for a general system of this type.³ Following his method, we have calculated the effect a WLC would have on such a system. Figure 1 shows the frequency response of a system with the parameters used in reference 3 with and without a WLC. Line A shows the frequency response when no signal recycling mirror is present. Line B shows the frequency response with a signal recycling mirror having transmissivity $T^2=0.25$, and no WLC. Note that this has a higher peak sensitivity and lower bandwidth, when compared to the broadband response shown in line A. Line D shows the frequency response with a signal recycling mirror having transmissivity $T^2=0.1$ and no WLC. The difference between lines B and D is simply that line D produces a higher sensitivity at the expense of reducing the bandwidth. This trade-off could be extended further by making the bandwidth increasingly narrow, while increasing the sensitivity. Line C shows the frequency response with a signal recycling mirror having transmissivity $T^2=0.25$, using the WLC. This is the WLC-enhanced version of line B. Finally, line E, which is the WLC enhanced version of line D, shows the frequency response with a signal recycling mirror having transmissivity $T^2=0.1$.

As can be seen by comparing line B and line C, the WLC produces a sensitivity which is even higher than the that obtained in the narrowband mode without the WLC, and it is broadband. The increase in

sensitivity compared to the narrowband case is a minor effect due to the fact that for the WLC both sidebands resonate at the same time. Of course, the same conclusion applies when comparing lines D and E. Without the WLC there is a clear trade-off between the bandwidth and the sensitivity, which constrains the maximum sensitivity during the narrowband mode operation. However, as is evident from these plots, the WLC eliminates this trade-off so that the sensitivity could actually be much higher than what is otherwise practical in the narrowband mode.

[Insert Figure 1 about here]

In reference 3, Meers proposes a scheme which he calls “dual recycling,” which simpler than that currently being considered for Advanced Ligo. The input test mass mirrors are not present; however, the signal recycling mirror is still used. This configuration may in fact be more practically suited to the use of a WLC. This design is less complex than the SEC scheme, requiring fewer control signals and fewer optical components in the arms, due to the absence of input test mass mirrors. Moreover, in this configuration, the fast-light medium can be placed outside the arms of the interferometer, which helps ensure that the arms themselves are as identical as possible. On the other hand, if the input test mass mirrors are present, the fast-light medium must be placed between those mirrors and the end test masses. Unlike the SEC scheme, the dual-recycling scheme does not allow us to control the output coupler reflectivity while the device is in operation. However, with a WLC, the need to reduce that reflectivity is obviated.

The only advantage to the broadband mode proposed for Advanced LIGO which cannot be achieved in this configuration has to do with the thermal properties of the optics. With an SEC set to a low reflectivity, the arm cavity length can be adjusted such that the carrier frequency resonates, allowing a high build-up of the carrier in the arms, which in turn increases the amplitudes of the sidebands. The sidebands do not resonate strongly in this cavity because of the low reflectivity of the SEC, which allows them to transmit out, while the carrier builds up. This allows the carrier intensity to be very high, while keeping the power on the main beamsplitter low, reducing thermal distortion and noise issues. In the absence of input test mass mirrors, the only way to build up the carrier field in the arms is to use a power recycling mirror at the bright port, which produces a high power level on the beamsplitter. The power in the carrier-frequency field is thus limited by the thermal properties of the beamsplitter in this configuration.

The WLC may also be implemented in the SEC scheme, avoiding these thermal issues. We will present a more thorough analysis of such a system in a future paper. These two detector designs, Advanced LIGO and the variation thereof with no input test mass mirrors, benefit equally from the WLC, although each has other advantages and disadvantages as described above. But while these are perhaps the best-developed designs, they are not the only possibilities. One competing design is a zero-area Sagnac interferometer based GW detector^{18,19,20}.

In the following sections, we propose a novel type of GW detector using a fast-light material that can have a strain sensitivity as much as a factor of 10^5 higher than that of the current LIGO type detectors. This idea builds on previous theoretical and experimental work on zero-area Sagnac interferometers and a proposal by Karapetyan²¹ for a version of the Michelson Interferometer based GW detector that increases its sensitivity by using amplifying mirrors that employ the same fast-light based effect. The enhanced sensitivity is based on the use of the fast-light effect, which results from negative dispersion.

We consider a variation of the zero-area Sagnac interferometer (ZASI) for GW detection, as originally proposed in references 19 and 20, discussed by us in reference 22 and studied experimentally in reference 18. In particular, we first replace the Sagnac interferometer with a Sagnac ring resonator, by changing the orientation of the beam-splitter at the input. This configuration --- a passive, zero-area Sagnac ring resonator (ZASRR) --- will increase the amplitude of the sideband by a factor equaling the finesse of the resulting

cavity (this cavity-induced enhancement --- CIE --- is akin to the kind of enhancement achieved by signal recycling, for example, and is *not* the fast-light induced enhancement). We then add, inside this cavity, a medium with negative dispersion, with parameters chosen to correspond to the WLC condition. However, as described later in this paper, this configuration --- a fast-light enhanced, passive ZASRR --- *does not* correspond to any enhancement in sensitivity; it simply enhances the bandwidth-sensitivity product of the detector, by increasing the bandwidth without decreasing the sensitivity.

Consider next a configuration where the passive ZASRR is made into an active ZASRR, by adding a gain medium inside the cavity. In the absence of the negative dispersive medium, this device has essentially the same sensitivity as that of the passive ZASRR, except that the CIE now is given by the square-root of the finesse of the active cavity at the sideband frequency, which can be considerably higher than the finesse of the passive cavity. We now add, inside the cavity, a medium with negative dispersion, with parameters chosen to correspond to the WLC condition. Of course, the WLC condition in this case will be different from that for the passive cavity, since one must also take into account any residual dispersion from the saturated gain medium. Under this condition, we show that the sideband amplitude is enhanced further by a factor that equals the inverse of the group index. Since the group index approaches a null value for the WLC condition, the fast-light induced enhancement --- FIE --- approaches infinity. However, due to higher order effects in the negative dispersion medium¹⁵, the actual FIE factor is limited to a finite value, which can be as high as 10^5 for parameters achievable practically. Since the signal is detected by monitoring the beat between the main laser mode and the sidebands, the cavity broadening effect does not affect the observed signal, as discussed in references 8 and 23.

[insert Figure 2 about here]

The rest of this paper is organized as follows. In Section III, we review the zero-area Sagnac interferometer for GW detection, comparing its properties against the more conventional GW detector based on a Michelson interferometer. In Section IV, we describe a modified version of such a detector where the Sagnac interferometer is replaced by a zero-area Sagnac ring resonator fed by an external laser. We also consider what happens if such a system is turned into a WLC. In Section V, we describe a GW detector based on an active, zero-area Sagnac ring resonator, where a gain medium is present inside the cavity. We then show that if the resonator is turned into a WLC by adding a negative dispersion material, then its sensitivity to GW strain is enhanced by the inverse of the group index of the dispersive medium. We describe conditions under which this enhancement factor could be as large as 10^5 . Finally, we add some concluding remarks in Section VI.

III. Review of Zero-Area Sagnac Interferometer vs. Michelson Interferometer for GW Detection

Figure 2 shows schematically a Michelson Interferometer (MI) usable for GW detection. Here, we assume that the beam splitter splits an input beam with equal amplitudes in each arm, and each arm has the same length, L , with a small offset introduced to ensure that the detector port is dark for the pump beam. If we assume the presence of a gravitational wave at a frequency of ω_g , with a small strain amplitude of h , then the differential space and time elements are related by the following equation:

$$dz^2 = c^2[1 + h \cos(\omega_g t)]dt^2 \quad (\text{eqn. 1})$$

which, in turn, implies that

$$dz \approx c[1 + \frac{h}{2} \text{Cos}(\mathbf{w}_g t)]dt \quad . \quad (\text{eqn. 2})$$

This relation corresponds to a differential phase shift of $d\mathbf{f}_1$ in arm 1, and $d\mathbf{f}_2$ in arm 2:

$$d\mathbf{f}_1 = -d\mathbf{f}_2 = \frac{wh}{2} \int_{t-\tau}^t \text{Cos}(\mathbf{w}_g t') dt' \quad (\text{eqn. 3})$$

[Insert Figure 3 about here]

Here, τ is the round-trip travel time in each arm. This phase shift produces a pair of sidebands, each with an amplitude that is proportional to $|d\mathbf{f}_1| = |d\mathbf{f}_2|$, but are opposite in sign. In the detector port, these two phase shifted beam add, producing a pair of sidebands, each with an amplitude equaling E_{GSB} , given by:

$$\frac{E_{GSB}}{E_o} = |\Delta\mathbf{f}| = 2|d\mathbf{f}_1| = 2|d\mathbf{f}_2| = \frac{wh}{\mathbf{w}_g} \text{Sin}(\mathbf{w}_g \mathbf{t} / 2) \quad (\text{eqn. 4})$$

where E_o is the amplitude of the pump field.

Figure 3 shows the Sagnac Interferometer for GW detection. Here, we again assume that τ is the roundtrip travel time on each leg, each leg has the same path length, L , and the beam splitter splits an input beam with equal amplitudes in each arm. The configuration is designed to ensure that the area covered by a beam traversing both legs is zero, so that it is not sensitive to rotation. The signal produced by this Zero-Area Sagnac Interferometer (ZASI) can be derived as follows. Briefly, the beams following the two paths (1 and 2, defined in Figure 3) undergo phase shifts $d\mathbf{f}_1$ and $d\mathbf{f}_2$, given by:

$$d\mathbf{f}_1 = -d\mathbf{f}_2 = \frac{wh}{2} \left[\int_{t-2\tau}^{t-\tau} \text{Cos}(\mathbf{w}_g t') dt' - \int_{t-\tau}^t \text{Cos}(\mathbf{w}_g t') dt' \right] \quad (\text{eqn. 5})$$

Here, again, τ is the round-trip travel time in each arm. This phase shift produces a pair of sidebands, each with an amplitude that is proportional to $|d\mathbf{f}_1| = |d\mathbf{f}_2|$, but are opposite in sign. Just as in the case of the MI, the detector port is configured to be dark for the pump. In the detector port, these two phase shifted beam add, producing a pair of sidebands, each with an amplitude equaling E_{GSB} , given by:

$$\frac{E_{GSB}}{E_o} = |\Delta\mathbf{f}| = 2|d\mathbf{f}_1| = 2|d\mathbf{f}_2| = \frac{2wh}{\mathbf{w}_g} \text{Sin}^2(\mathbf{w}_g \mathbf{t} / 2) \quad (\text{eqn. 6})$$

[Insert Figure 4 about here]

Note that the response of this detector is different from that of the MI, both qualitatively and quantitatively. For example, in the case of the ZASI, in the limit of very small frequencies ((i.e., $\mathbf{w}_g \ll 1/\mathbf{t}$), the sideband amplitude is proportional to \mathbf{w}_g . As such, the sensitivity of this detector is peaked at a non-zero value. In contrast, the MI configuration has the property that for very small frequencies (i.e., $\mathbf{w}_g \ll 1/\mathbf{t}$), the amplitude

of the sidebands is essentially independent of the frequency. This is illustrated in Figure 4. Here we have assumed $h = 10^{-23}$, $w \approx 1.8 \cdot 10^{15}$ corresponding to the Nd:YAG laser, and $L_{(effective)} = 160 \text{ km}$, which corresponds to a physical length for each arm of $L = 4 \text{ km}$, and 20 bounces in each term. The bounces can be realized by optical delay lines; alternatively, a Fabry-Perot cavity can be used in each arm to produce an effect equivalent to the multiple bounces. The later approach is used in the LIGO type observatories, for example.

If this approach is used, the WLC can broaden the detection bandwidth in exactly the same way described in section II for the Advanced LIGO configuration—the arm cavities can resonate any GW induced sideband, in the presence of an appropriately dispersive medium.

This configuration for GWD has a set of potential advantages compared to the MI, as discussed in reference 25. Specifically, this interferometer is insensitive to laser frequency variation, mirror displacement at dc, thermally induced birefringence, and reflectivity imbalance in the arms, allowing a simplified control system and reduced optical tolerance requirements.

IV. Overview of Passive, Zero-Area Sagnac Ring Resonator for GW Detection

The ZASI can be reconfigured as a resonator, thus realizing a passive, Zero-Area Sagnac Ring Resonator (ZASRR) for gravitational wave detection. This is illustrated schematically in Figure 5.

[Insert Figure 5 about here]

Here, the input beam splitter is rotated by ninety degrees from the ZASI orientation. Furthermore, it has a high reflectivity, R , which approaches unity in order to produce a high-finesse resonator. Here, the beams are propagating only along path 2 (defined in Figure 3). The response of the ZASRR can be determined by considering the multiple bounces at the beam splitter experienced by the sidebands produced during the first trip, in a manner analogous to the derivation of power and signal recycling in reference 3. Note that this is a one-sided cavity on reflection; the behavior of such a cavity is analyzed, for example, in reference 6. The end result is that each of the two sidebands in the detector port has an amplitude of E_{GSB} given by:

$$\frac{E_{GSB}}{E_o} = F |d\mathbf{f}_2| = F \frac{wh}{w_g} \text{Sin}^2(w_g \tau / 2) \quad (\text{eqn. 7})$$

where τ again is the round-trip time for each leg, E_o is the input pump field, and F is the finesse of the ring resonator:

$$F = p\sqrt{R}/(1-R). \quad (\text{eqn. 8})$$

Here, we have assumed that the cavity is broad enough so that both the pump and the sidebands resonate. Therefore, the pump gets amplified by a factor of \sqrt{F} . Each sideband also gets amplified by the same factor of \sqrt{F} . Therefore, the net cavity induced enhancement (CIE) factor is F . Under these assumptions, both the pump field (with amplitude of E_o) and the sidebands are present in the detector port. The signal can be observed by mixing the pump and the sidebands on the detector, and looking at the beat spectrum.

Consider now a situation where a material with negative dispersion is placed inside the cavity, with parameters chosen so that the resonator behaves as a WLC. Under this condition, it is easy to show, using the

model discussed in references 8 and 15, that the cavity bandwidth will be increased, without any decrease in the cavity finesse. As such, it would be possible to detect GWs with a larger sensitivity-bandwidth product than what is achievable with the empty cavity. This effect is akin to the enhancement of the bandwidth-sensitivity product of the type considered in reference 8 and 24. However, for reasons that would be evident after the discussion in Section IV, there is no Fast-Light Induced Enhancement (FIE) in strain sensitivity in this case.

V. Fast-Light Enhanced, Active, Zero-Area Sagnac Ring Resonator for GW Detector

We now consider the case where a gain medium is placed inside the zero-area Sagnac ring resonator. This is illustrated in Figure 6. Here, we assume that a Faraday isolator is present inside the resonator, in order to ensure that the lasing action takes place in only one direction. This constitutes an active ZASRR configured as a gravitational wave detector. Using the same type of analysis as outlined above, we get that each sideband has an amplitude of E_{GSB} , given by:

$$\frac{E_{GSB}}{E_o} = \sqrt{F_{SB}} |\Delta f| = \sqrt{F_{SB}} \frac{2wh}{w_g} \text{Sin}^2(w_g t / 2) \quad (\text{eqn. 9})$$

Here again, τ is the round-trip travel time for each leg, E_o is the amplitude of the laser field inside the resonator, and F_{SB} is the active finesse of the gain-saturated cavity at the sideband frequencies. As before, we assume that the cavity is broad enough for both the

[Insert Figure 6 about here]

laser and the sidebands to resonate simultaneously. Here, the sidebands resonate as if they are in a passive cavity, except that the effective reflectivity of the beam splitter is increased due to the fact that there is residual gain that offsets the loss at the beamsplitter, in order to ensure steady-state operation of the laser mode. As such, the active finesse is much higher than the passive finesse. As in the case of the passive cavity, the output contains both the main laser field amplitude, given by $E_o \sqrt{(1-R)}$, and the sidebands. These signals are mixed on a detector, and the beat note spectrum is monitored as the signature of gravity waves.

We now consider the situation where a negative dispersive medium is inserted in the cavity. This is illustrated in Figure 7, where the dispersive medium is denoted as the WLC-DE (White Light Cavity Dispersive Element). The parameters are chosen to ensure the WLC condition. Note that in this case the residual dispersion of the gain medium also has to be taken into account in order to determine the overall negative dispersion inside the cavity. This constitutes the fast-light enhanced, active ZASRR as a gravitational wave detector.

To determine the response of this detector, let us recall first the process of enhanced sensitivity to displacement in a WLC, as described in reference 15. Briefly, consider first a (passive) cavity without any dispersive material inside, tuned to resonance at frequency w_o . If the cavity length now changes by an amount ΔL , the cavity can be restored to resonance by adjusting the frequency of the light by amount Δw_o . Consider next the same process in the presence of a negative dispersion material satisfying the condition for WLC. In this case, the amount of frequency change needed to restore resonance is given by:

$$\Delta \mathbf{w} = \mathbf{x} \Delta \mathbf{w}_o . \quad (\text{eqn. 10})$$

[Insert Figure 7 about here]

For non-vanishing values of n_g , the group index, the enhancement factor, ξ is given by $1/n_g$. As $n_g \rightarrow 0$, higher order non-linearities in the dispersion profile becomes relevant, thus avoiding divergence, as discussed in detail in reference 15. For example, if a system (such as the one we used to demonstrate WLC in reference 8) with a negative dispersion width of $\Gamma \approx 2\mathbf{p} \times 10^6 \text{ sec}^{-1}$ is used, the need for taking higher-order non-linearity into account occurs for $n_g \leq 10^{-5}$. In this range, the enhancement factor is given approximately by 15 :

$$\mathbf{x} = [2\Gamma / \Delta \mathbf{w}_o]^{2/3} \quad (\text{eqn. 11})$$

Note that this factor is non-linear, and depends on the value of $\Delta \mathbf{w}_o$ itself. In the case of applying the WLC-enhancement to rotation sensing, it is fine to operate in a regime where eqn. 11 is valid, since the actual rotation rate can be easily surmised by inverting equations. 10 and 11. For the case of GWD, such an inversion is potentially more cumbersome, except possibly in the case of a purely monochromatic gravitational wave. As such, the application of the fast-light induced enhancement to the strain sensitivity should be limited to the regime where the value of ξ is simply given by $1/n_g$, independent of the value of $\Delta \mathbf{w}_o$.

Consider now the active ZASRR. The effect of the GW is to change the cavity length, as given by eqn. 2. Since a typical GW is very slow as compared to the response time of the laser cavity, the GW induced change in the cavity length can be considered as an adiabatic process. Therefore, the laser frequency gets continuously adjusted, automatically, in order to compensate for the GW induced change in the cavity length. In the absence of the dispersive medium, the resulting $\Delta \mathbf{w}_o$, as a function of time, is simply given by:

$$\Delta \mathbf{w}_o(t) = \frac{\mathbf{w}h}{2} \text{Cos}(\mathbf{w}_g t) \quad (\text{eqn. 12})$$

so that the phase shift produced can be expressed as:

$$\Delta \mathbf{f} = \int_{t-t}^t \frac{\mathbf{w}h}{2} \text{Cos}(\mathbf{w}_g t') dt' = \int_{t-t}^t \Delta \mathbf{w}_o dt' . \quad (\text{eqn. 13})$$

Note that eqn. 12 can be understood simply from the relation that

$$\frac{\Delta \mathbf{w}_o}{\mathbf{w}} = \frac{\Delta L}{L} \approx \frac{h}{2} \text{Cos}(\mathbf{w}_g t). \quad (\text{eqn. 14})$$

In the presence of the negative dispersion material satisfying the WLC condition, the value of the frequency correction is now given by

$$\Delta \mathbf{w} = \mathbf{x} \Delta \mathbf{w}_o(t) = \mathbf{x} \frac{\mathbf{w}h}{2} \text{Cos}(\mathbf{w}_g t) \quad (\text{eqn. 15})$$

so that the phase shift produced is given by:

$$\Delta \mathbf{f}_{ENH} = \int_{t-t}^t \Delta \mathbf{w} dt' = \int_{t-t}^t \mathbf{x} \Delta \mathbf{w}_o dt' = \int_{t-t}^t \mathbf{x} \frac{\mathbf{w}h}{2} \text{Cos}(\mathbf{w}_g t') dt' \quad (\text{eqn. 16})$$

which, in turn, implies that the sideband amplitude is also amplified by the ξ factor:

$$\frac{E_{GSB}}{E_o} = \mathbf{x} \sqrt{F_{SB}} |\Delta \mathbf{f}| = \mathbf{x} \sqrt{F_{SB}} \frac{2\mathbf{w}h}{\mathbf{w}_g} \text{Sin}^2(\mathbf{w}_g t / 2) \quad (\text{eqn. 17})$$

As noted above, we have assumed here that the FIE factor, ξ , is a constant, given by $1/n_g$, and is independent of $\Delta \mathbf{w}_o$. As such, for the case of a resonant negative dispersion linewidth of $\Gamma \approx 2\mathbf{p} \cdot 10^6 \text{ sec}^{-1}$, the FIE factor is $\cong 10^5$.

We point out that a similar result was derived in reference 21 by Karapetyan. However, the configuration considered in reference 21 is markedly different from what we have proposed here. Specifically, he considers the use of a linear, white-light cavity as a mirror in a linear interferometer. Furthermore, he does not address the issue of detection that allows one to overcome the effect of line-broadening in the WLC.

VI. Conclusion and Discussion

Equation 17 is the key result of this paper. To summarize, it shows that the strain sensitivity is enhanced effectively by a factor of nearly 10^5 . This is over and above the active cavity induced enhancement of $\sqrt{F_{SB}}$. Of course, enhancement of sensitivity by itself does not necessarily mean that we can detect smaller strains. What matters is an effective enhancement in the signal to noise ratio (SNR). Given that a gain medium is present, and an additional medium is used to produce the FIE, it is plausible that some excess noise may get introduced into the system. However, it is unlikely that these additional sources of noise would swamp the enhancement. To see why, we note that one of the most sensitive optical sensor is a ring laser gyroscope (RLG), which makes use of a ring resonator of the type employed here. The RLG is capable of producing fundamental quantum noise limited performance due in large part to the fact that the observed signal is a beat between two lasing modes that share the same cavity. As such, all excess noise is cancelled out. In detailed analyses^{23,25} carried out by us, taking into account real system parameters, we have shown that a WLC-augmented RLG is also capable of quantum-noise limited performance, so that the WLC induced enhancement to rotational sensitivity leads to a corresponding enhancement in the SNR. The same conclusion should also apply here. Therefore, we expect that the SNR will be enhanced by the factor of $\mathbf{x} \cong 10^5$. However, the beat employed here is between the fundamental mode and the sidebands, which is different from what happens in an RLG. As such, subtle differences may arise in the way excess noise is suppressed in this case. Theoretical analysis akin to reference 23 have to be carried out to address this issue explicitly. However, these differences are not likely to affect significantly the fundamental enhancement expected from using this configuration.

Of course, the ideas presented here must first be tested experimentally before one considers constructing a GW detector based on these principles. Such an experiment can be carried out using a zero-area Sagnac ring laser using a Ti:Sapphire crystal, and a Raman-pumped Rubidium vapor cell can be used to produce the negative dispersion. An electro-optic modulator can be employed to mimic the effect of GW, as has often been done in testing the technologies behind the LIGO type observatories. We also note that the configuration considered here is potentially consistent with the optical components and the vacuum system currently used by LIGO-type observatories. For making use of the LIGO optical components, Nd:YAG could be used as the gain medium for the ring laser, and a pumped photorefractive crystal could be used to produce the negative dispersion. We have recently shown experimentally²⁶ and theoretically²⁷ the viability of using such a crystal for making a WLC.

Whether the next generation of gravitational wave detectors uses the Advanced LIGO scheme, a signal recycling scheme without input test masses, a Sagnac interferometer or a Sagnac resonator, the WLC concept has important potential applications, broadening the detection bandwidth without reducing sensitivity, and increasing the sensitivity by a factor of as much as a hundred thousand, depending on the configuration.

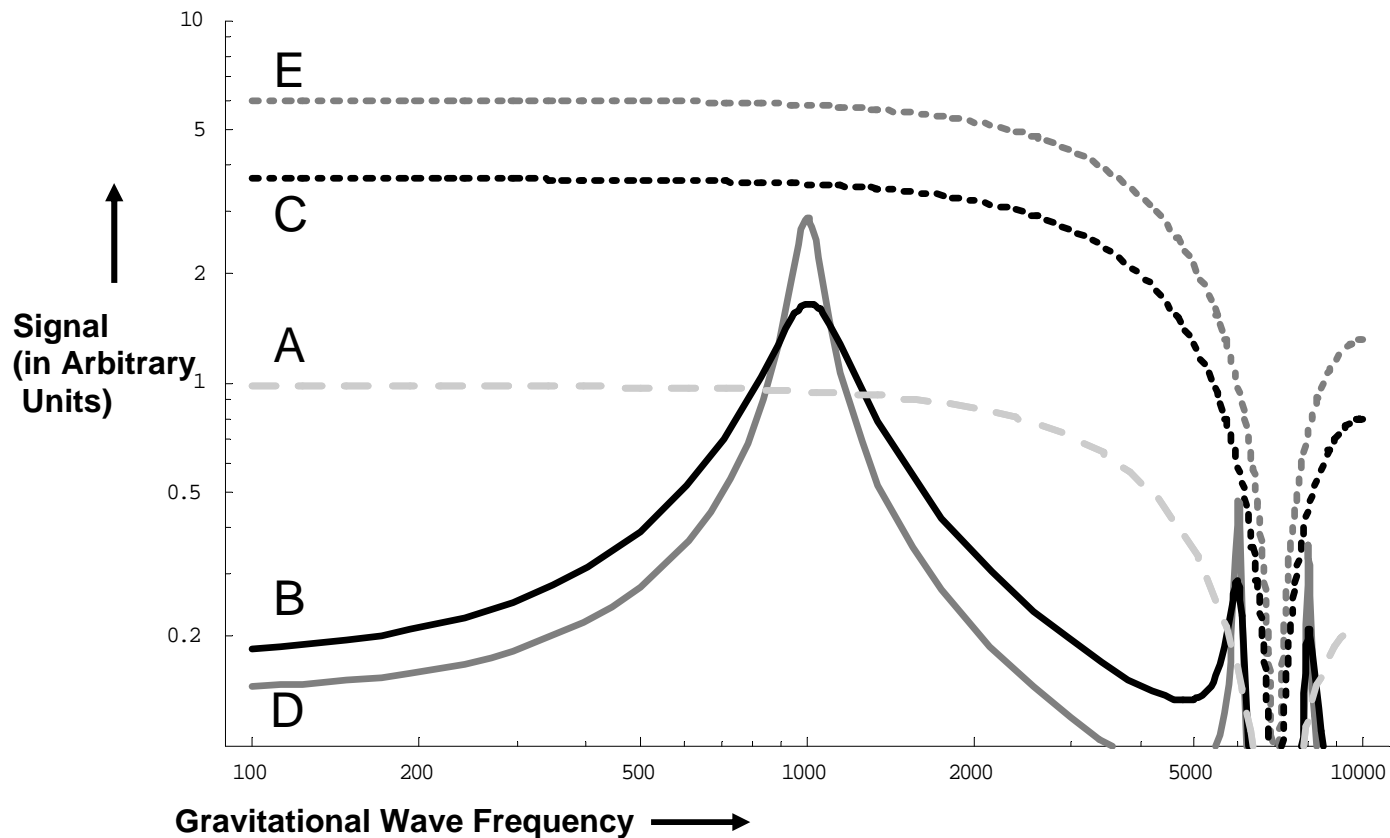


Figure 1: Effect of WLC on a system such as that modeled in reference 3. A) frequency response when no signal recycling mirror is present. B) Frequency response with a signal recycling mirror having transmissivity $T^2=0.25$, and no WLC C) Frequency response with a signal recycling mirror having transmissivity $T^2=0.25$, using the WLC D) Frequency response with a signal recycling mirror having transmissivity $T^2=0.1$ and no WLC E) Frequency response with a signal recycling mirror having transmissivity $T^2=0.1$, using the WLC.

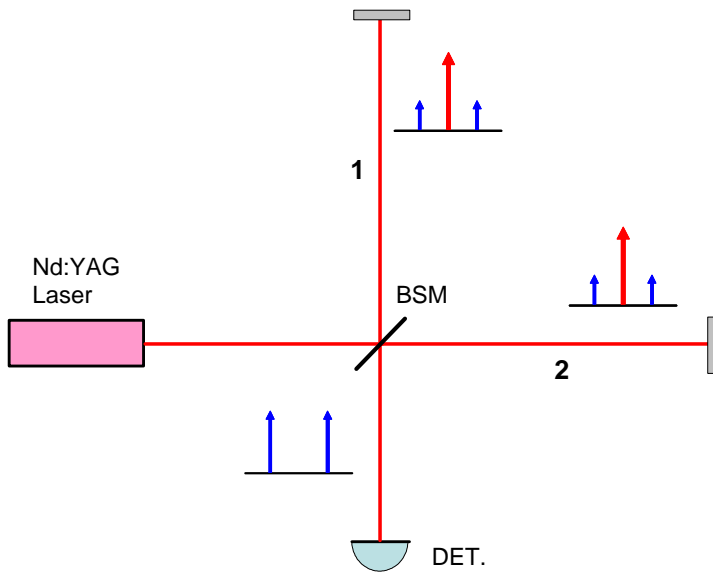


Figure 2: Schematic illustration of a basic Michelson Interferometer for GWD. Here, we assume that each arm has the same length, with an offset introduced to ensure that the detector port is dark for the pump beam.

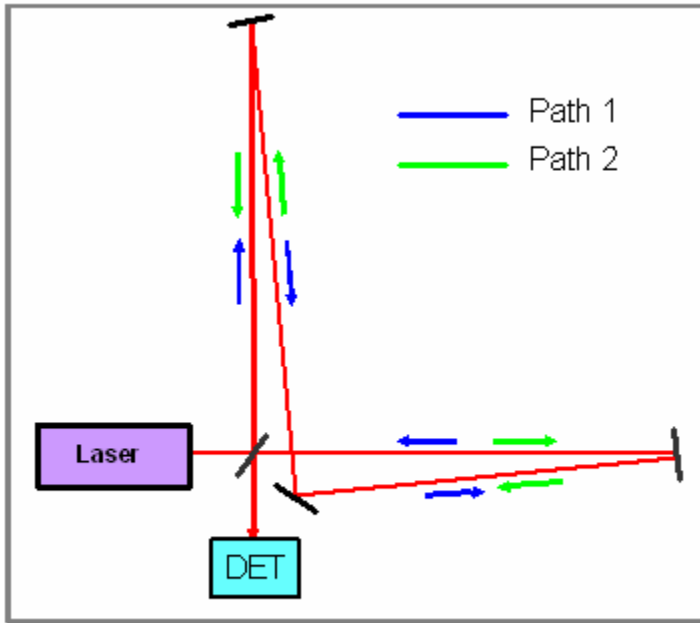


Figure 3: Schematic illustration of the Sagnac Interferometer gravitational wave detection. Here, the net area enclosed by a beam traversing both arms is zero, thus making it insensitive to rotation. We assume each arm has the same length L . See text for additional details.

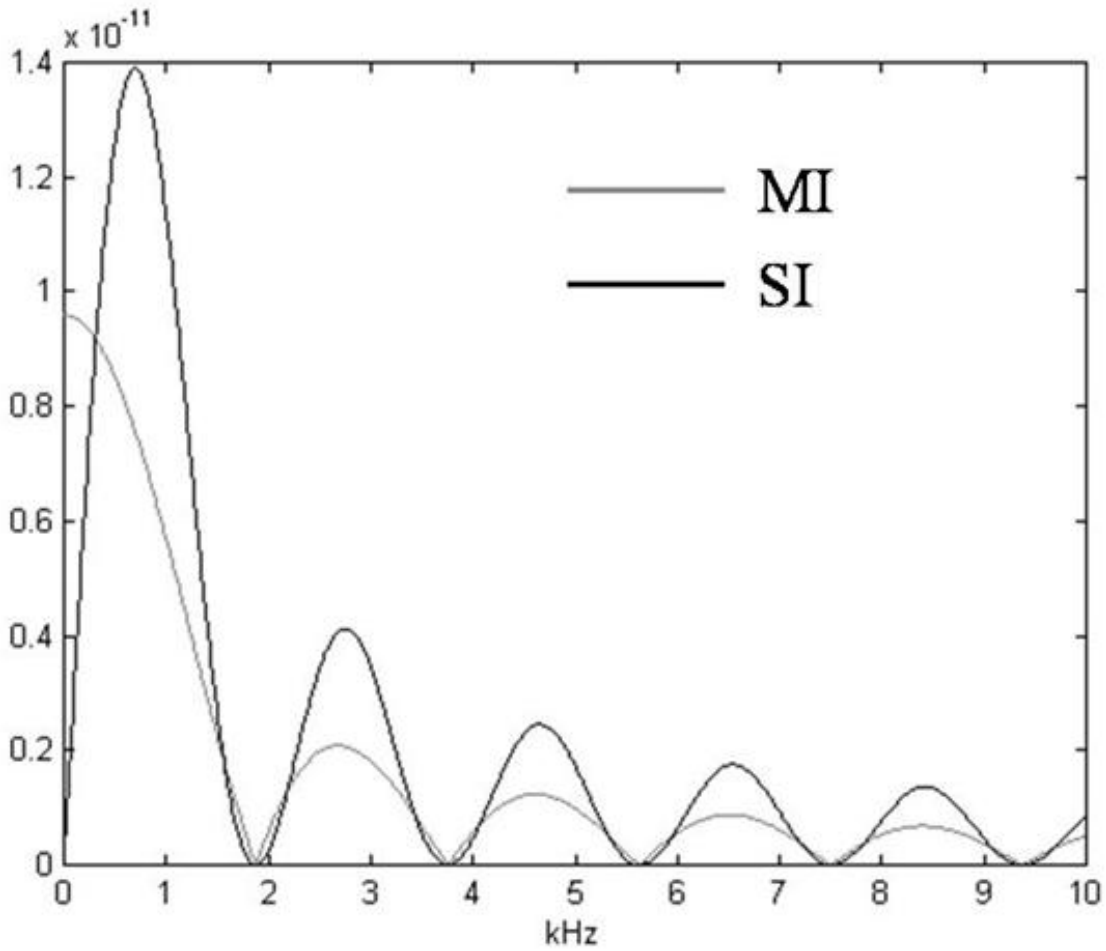


Figure 4: Plots of fractional sideband amplitudes vs. gravitational wave frequency for the Michelson Interferometer (light) and the zero-area Sagnac Interferometer (dark). Note that for the Sagnac Interferometer, the sensitivity peaks at a non-zero frequency of gravitational waves. See text for details.

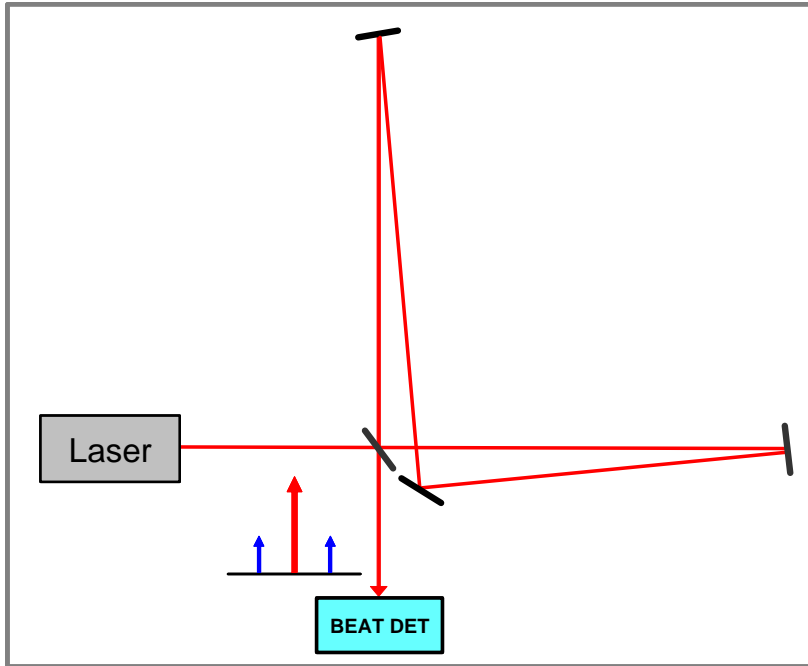


Figure 5: Schematic illustration of a passive, zero-area Sagnac ring resonator (ZASRR) for gravitational wave detection. See text for details.

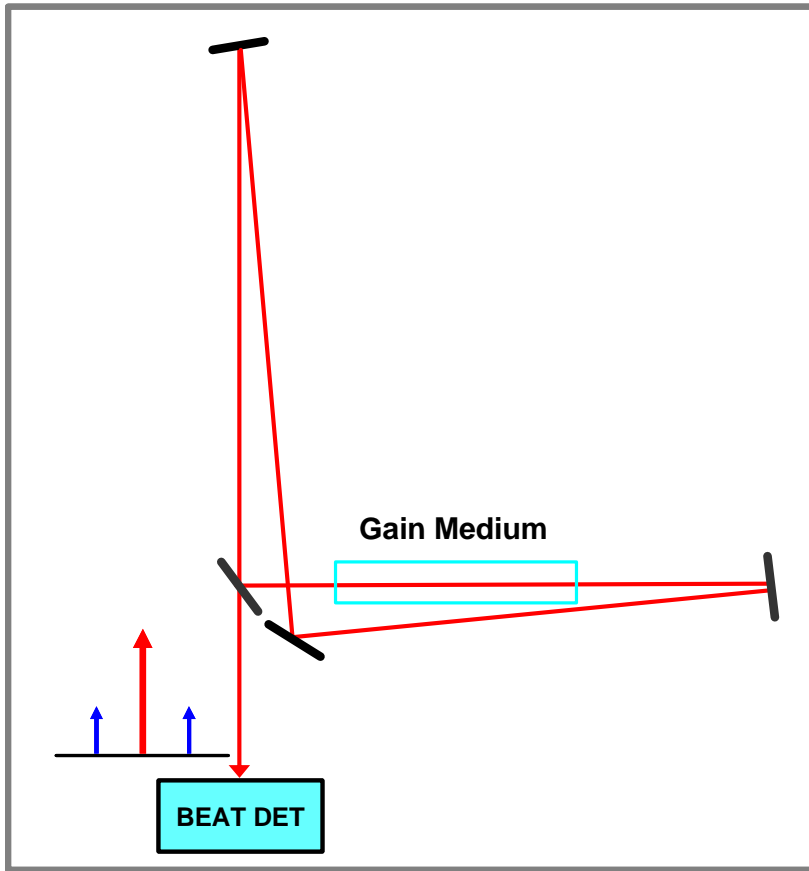


Figure 6: Schematic illustration of the active, zero-area Sagnac ring resonator as a gravitational wave detector. See text for details.

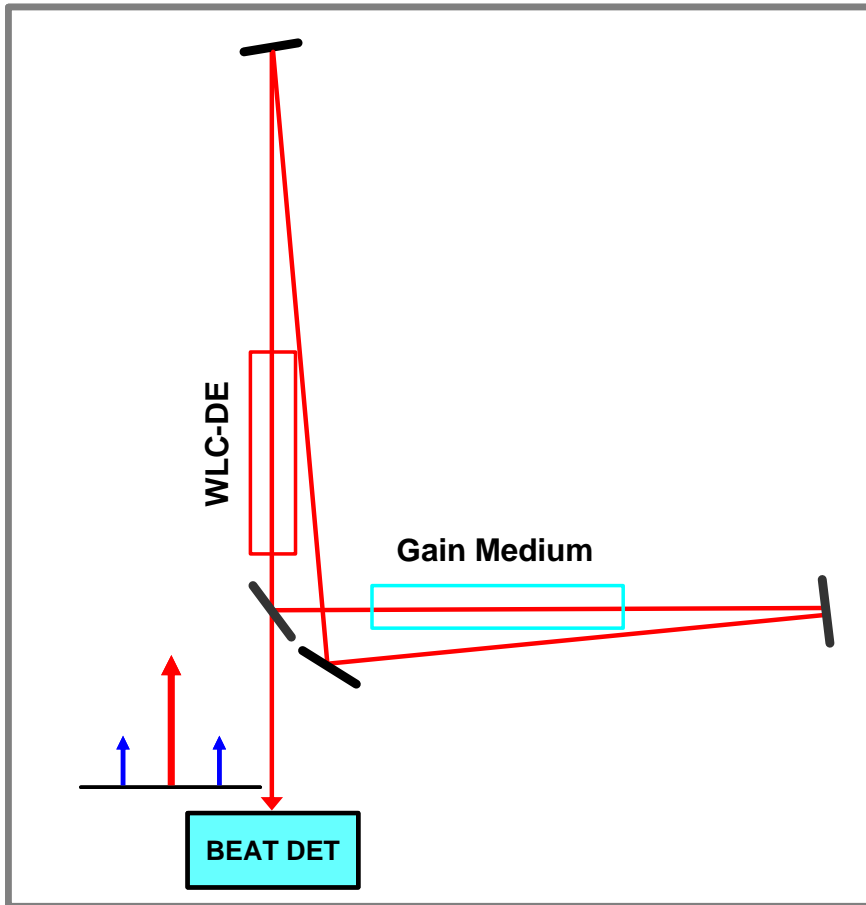


Figure 7: Schematic illustration of the fast-light enhanced, active, zero-area Sagnac ring resonator as a gravitational wave detector. See text for details.

-
- ¹ The Detection of Gravitational Waves, ed. D.G. Blair (Cambridge University Press, Cambridge, 1991).
- ² K. Danzmann and A. Rudiger, "Seeing the universe in the light of gravitational waves", *Rev. Mod. Astron.* 15, 212 (2002).
- ³ B.J. Meers, "Recycling in laser-interferometric gravitational-wave detectors", *Phys. Rev. D* 38, 2317 (1988).
- ⁴ G. Heinzel, K.A. Strain, J. Mizuno, K. D. Skeldon, B. Willke, W. Winkler, R. Schilling, A. Rüdiger and K. Danzmann, "Experimental demonstration of a suspended dual recycling Interferometer for gravitational wave detection", *Phys. Rev. Lett.* 81, 5493 (1998).
- ⁵ M.B. Gray, A.J. Stevenson, H-A Bachor, D.E. McClelland, "Broadband and tuned signal recycling with a simple Michelson interferometer", *Appl. Opt.* 37, 5886 (1998).
- ⁶ E.D. Black, R. N. Gutenkunst, "An introduction to signal extraction in interferometric gravitational wave detectors", *Am. J. Phys.* 71, 365 (2003).
- ⁷ T.T. Lyons, M.W. Regehr, F.J. Raab, "Shot noise in gravitational-wave detectors with Fabry-Perot arms", *Appl. Opt.* 39, 6761 (2000).
- ⁸ G. S. Pati, M. Salit, K. Salit, and M. S. Shahriar, "Demonstration of a Tunable-Bandwidth White-Light Interferometer Using Anomalous Dispersion in Atomic Vapor", *Phys. Rev. Lett.* **99**, 133601 (2007)
- ⁹ A. Dogariu, A. Kuzmich, and L. J. Wang "Transparent anomalous dispersion and superluminal light-pulse propagation at a negative group velocity", *Phys. Rev. A* 63, 053806 (2001)
- ¹⁰ A. Wicht, K. Danzmann, M. Fleischhauer, M. Scully, G. Müller, R.H. Rinkleff, "White-light cavities, atomic phase coherence, and gravitational wave detectors", *Opt. Commun.* 134, 431 (1997).
- ¹¹ A. Rocco, A. Wicht, R.H. Rinkleff, K. Danzmann, "Anomalous dispersion of transparent atomic two- and three level ensembles", *Phys. Rev. A* 66, 053804 (2002).
- ¹² R.H. Rinkleff, A. Wicht, "The concept of white light cavities using atomic phase coherence", *Physica Scripta T118*, 85 (2005).
- ¹³ S. Wise, G. Mueller, D. Reitze, D.B. Tanner, B.F. Whiting, "Linewidth-broadened Fabry–Perot cavities within future gravitational wave detectors", *Class. Quant. Grav.* 21, S1031 (2004).
- ¹⁴ S. Wise, V. Quetschke, A. J. Deshpande, G. Mueller, D.H. Reitze, D. B. Tanner, B. F. Whiting, Y. Chen, A. Tunnermann, E. Kley, T. Clausnitzer, "Phase effects in the diffraction of light: Beyond the grating equation", *Phys. Rev. Lett.* 95, 013901 (2005).
- ¹⁵ M.S. Shahriar, G.S. Pati, R. Tripathi, V. Gopal, M. Messall, "Ultrahigh precision rotation sensing using a fast-light enhanced ring laser gyroscope", *Phys. Rev. A* 75, 053807 (2007).
- ¹⁶ G.S. Pati, M. Messall, K. Salit, M.S. Shahriar, "Demonstration of tunable displacement- measurement-sensitivity using variable group index in a ring resonator", *Optics Communications* 281 (2008) 4931–4935.
- ¹⁷ G.S. Pati, M. Messall, K. Salit, M.S. Shahriar, "Demonstration of tunable displacement- measurement-sensitivity using variable group index in a ring resonator", proceedings of SPIE Photonics West, Jan. 2007, San Jose, CA.

- ¹⁸ K-X Sun, M. M. Fejer, E. Gustafson, R. L. Byer. “Sagnac interferometer for gravitational-wave detection”, *Phys. Rev. Lett.* 76, 17 (1996).
- ¹⁹ R. W. P. Drever, in “Gravitational Radiation”, edited by N. Deruelle and T. Piran (North-Holland, Amsterdam, 1983)
- ²⁰ R. Weiss, in NSF Proposal, 1987.
- ²¹ G.G. Karapetyan, “Advanced configuration of gravitational-wave interferometer on the base of sensitive mode in white-light cavity” *Opt. Commun.* 219, 335 (2003).
- ²² M.S. Shahriar, M. Salit, “Anomalous-dispersion enhanced active sagnac interferometry for gravitational wave detection”, *Proceedings of SPIE Photonics West*, Feb, 2008
- ²³ M.S. Shahriar, M. Salit, and J.H. Shapiro, “Model for beat noise in a fast-light enhanced ring laser gyroscope”, (<http://lapt.eecs.northwestern.edu/preprints/beat-noise-in-FRLG.pdf>)
- ²⁴ M. Salit, G. S. Pati, K. Salit, and M. S. Shahriar, (2007) 'Fast-light for astrophysics: super-sensitive gyroscopes and gravitational wave detectors', *Journal of Modern Optics*, 54:16, 2425 – 2440.
- ²⁵ Q. Sun, M. S. Shahriar, M. S. Zubairy, “Effects of parameter variations and noises on a double-Raman white light cavity”, (<http://lapt.eecs.northwestern.edu/preprints/noise-in-double-raman-wlc.pdf>)
- ²⁶ G.S. Pati, M. Salit, S. Tseng, and M.S. Shahriar, “Demonstration of negative dispersion for a white light cavity using a BTO crystal with two pumps and a probe”, (<http://lapt.eecs.northwestern.edu/preprints/demo-bto-for-wlc.pdf>)
- ²⁷ Q. Sun, M. S. Shahriar, M. S. Zubairy, “Slow light and fast light in a photorefractive crystal”, (<http://lapt.eecs.northwestern.edu/preprints/slow-fast-prc.pdf>)